

Variable Contributions of Basic Residues Forming an APC Exosite in the Binding and Inactivation of Factor VIIIa

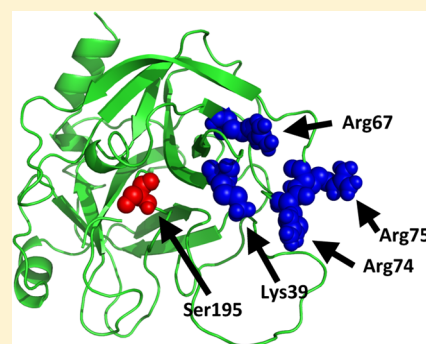
Masahiro Takeyama,^{†,§} Jennifer M. Wintermute,[†] Chandrashekhara Manithody,[‡] Alireza R. Rezaie,[‡] and Philip J. Fay^{*,†}

[†]Department of Biochemistry and Biophysics, University of Rochester School of Medicine and Dentistry, Rochester, New York 14642, United States

[‡]Edward A. Doisy Department of Biochemistry and Molecular Biology, Saint Louis University School of Medicine, Saint Louis, Missouri 63104, United States

S Supporting Information

ABSTRACT: Basic residues contained in the 39-, 60-, and 70–80-loops of activated protein C (APC) comprise an exosite that contributes to the binding and subsequent proteolytic inactivation of factor (F) VIIIa. Surface plasmon resonance (SPR) showed that WT APC bound to FVIII light chain (LC) and the FVIIIa A1/A3C1C2 dimer with equivalent affinity ($K_d = 525$ and 546 nM, respectively). These affinity values may reflect binding interactions to the acidic residue-rich a1 and a3 segments adjacent to A1 domain in the A1/A3C1C2 and A3 domain in LC, respectively. Results from SPR, using a panel of APC exosite variants where basic residues were mutated, in binding to immobilized FVIIIa A1/A3C1C2 or LC indicated ~4–10-fold increases in the K_d values relative to WT for several of the variants including Lys39Ala, Lys37-Lys38-Lys39/Pro-Gln-Glu, and Arg67Ala. On the other hand, a number of APC variants including Lys38Ala, Lys62Ala, and Lys78Ala showed little if any change in binding affinity to the FVIII substrates. FXa generation assays and Western blotting, used to monitor rates of FVIIIa inactivation and proteolysis at the primary cleavage site in the cofactor (Arg³³⁶), respectively, showed marked rate reductions relative to WT for the Lys39Ala, Lys37-Lys38-Lys39/Pro-Gln-Glu, Arg67Ala, and Arg74Ala variants. Furthermore, kinetic analysis monitoring FVIIIa inactivation by APC variants at varying FVIIIa substrate concentration showed ~2.6–4.4-fold increases in K_m values relative to WT. These results show a variable contribution of basic residues comprising the APC exosite, with significant contributions from Lys39, Arg67, and Arg74 to forming a FVIIIa-interactive site.



Factor VIII¹ functions as a cofactor for FIXa in the enzyme complex termed FXase that is responsible for the anionic phospholipid surface-dependent conversion of FX to FXa.¹ FVIII is synthesized as a multidomain (A1-a1-A2-a2-B-a3-A3-C1-C2), single chain molecule consisting of 2332 amino acid residues with a molecular mass of ~300 kDa. Domains are separated by short, acidic residue-rich regions designated by a lower case “a”. This precursor is processed to a series of divalent metal ion dependent heterodimers by cleavage at the B-A3 junction, generating a HC consisting of the A1-a1-A2-a2-B domains and a LC consisting of the a3-A3-C1-C2 domains.^{2–4} The procofactor FVIII is activated by cleavages at Arg³⁷², Arg⁷⁴⁰, and Arg¹⁶⁸⁹ by either thrombin or FXa, converting the heterodimer into the FVIIIa heterotrimer composed of the A1, A2, and A3C1C2 subunits.⁵ The A1 and A3C1C2 subunits are stably associated while the A2 subunit remains associated through weak electrostatic interaction. Proteolysis at Arg³⁷² and Arg¹⁶⁸⁹ is essential for generating FVIIIa cofactor activity. Cleavage at Arg³⁷² exposes a functional FIXa-interactive site within the A2 domain that is cryptic in the unactivated molecule.⁶ Cleavage at Arg¹⁶⁸⁹

liberates the cofactor from its carrier protein, VWF,⁷ and contributes to the overall specific activity of cofactor.⁸

The FXase complex is downregulated by two mechanisms that result in cofactor inactivation.⁹ One mechanism results from spontaneous decay of the A2 subunit from the A1/A3C1C2 dimer,¹⁰ although the association of FVIIIa in the FXase complex partially stabilizes interactions with A2 and reduces the dissociation rate of this subunit.¹⁰ The second mechanism results from proteolytic inactivation and is catalyzed by activated protein C (APC)^{5,11} or FXa.^{5,12} APC cleaves at Arg³³⁶ in the A1 subunit and Arg⁵⁶² in the A2 subunit of FVIIIa.^{11,13} Reaction at the former site occurs at an ~25-fold faster rate than at the latter site and correlates with the inactivation of FVIII/VIIIa.¹¹

The catalytic domain of APC possessing a trypsin-like primary specificity pocket is located on the C-terminal region of heavy chain. In the three-dimensional structure,^{14–16} the catalytic domain of APC contains several positively charged

Received: December 5, 2012

Revised: February 5, 2013

Published: March 12, 2013

residues that are clustered at a region on the right side of the active site. These basic residues are clustered in three conserved surface loops 39, 60, and 70–80. The primary binding between APC and FVIII is initiated by exosite-dependent interaction, and basic residues found in all three surface loops in APC appear to contribute to the interaction with FVIIIa.¹⁷

In the current study, we use a panel of point mutants where individual residues within the 39-, 60-, and 70–80-loops are replaced with Ala to assess potential contributions of each residue to FVIII-directed binding and catalysis. Binding studies employ two FVIII reagents: the FVIIIa-derived A1/A3C1C2 dimer and the isolated FVIII LC. Both substrates possess segments of acidic-rich residues, the a1 segment at the C-terminal end of the A1 domain in the A1/A3C1C3 dimer, and the a3 segment that precedes the A3 domain in the FVIII LC. Results from SPR, FXa generation, and Western blotting assays suggest variable contributions of residues in these loops to interactions with FVIII, with more prominent contributions attributed to APC residues Lys39, Arg67, and Arg74.

MATERIALS AND METHODS

Reagents. Recombinant FVIII (Kogenate) and the monoclonal antibody 58.12¹⁸ recognizing the N-terminal end of the A1 domain were generous gifts from Dr. Lisa Regan of Bayer Corp. (Berkeley, CA). The reagents human α -thrombin, FXa, human APC, and human APC-DEGR (Hematologic Technologies Inc., Essex Junction, VT), FIXa and FX (Enzyme Research Laboratory, South Bend, IN), hirudin (DiaPharma, West Chester, OH), the APC-specific chromogenic substrate, S-2366 (Chromogenix, Milano, Italy), and the chromogenic Xa substrate, Pefachrome Xa (Pefa-5523, CH₃OCO-D-CHA-Gly-Arg-pNA AcOH; Centerchem, Inc., Norwalk, CT) were purchased from the indicated vendors. Phospholipid vesicles (40% phosphatidylcholine (PC), 40% phosphatidylethanolamine (PE), and 20% phosphatidylserine (PS)) were prepared as described¹⁹ using phospholipids purchased from Avanti Polar Lipids Inc. (Alabaster, AL).

Mutagenesis, Expression and Purification of Recombinant Proteins. Recombinant wild-type FVIII was constructed, expressed, and purified as described previously.²⁰ Resultant FVIII was typically >90% pure as judged by SDS-PAGE with albumin representing the major contaminant. FVIII concentration was measured using an enzyme-linked immunosorbent assay (ELISA), and FVIII activity was determined by one-stage clotting assay and a two-stage chromogenic FXa generation assay. FVIII samples were quick-frozen and stored at –80 °C. Protein C derivatives in which the basic residues of the 39-loop (Lys38, Lys39), 60-loop (Lys62, Lys63, and Arg67), and 70–80-loop (Arg74, Arg75, and Lys78) were individually substituted with Ala were constructed, expressed, and purified as described previously.^{21,22} Furthermore, the three basic residues of the 39-loop (Lys37-Lys38-Lys39) were substituted with the homologous sequence of thrombin (Pro-Gln-Glu) to yield the triple mutant (Lys-Lys-Lys/Pro-Gln-Glu), which was prepared as described above. The wild-type and variant protein C mutants were expressed in HEK293 cells using the pRC/RSV expression vector (Invitrogen, San Diego, CA) as described.²¹ All protein C mutants were purified by immunoaffinity chromatography using the Ca²⁺-dependent monoclonal antibody, HPC4, linked to Affi-Gel 10 (Bio-Rad, Hercules, CA) as previously described.²¹

Isolation of Factor VIIIa Subunits. FVIII LC²³ and FVIIIa A1/A3C1C2 dimer²⁴ were isolated from recombinant FVIII (Kogenate) as previously described.

Protein C Activation. Protein C derivatives (1 mg) were incubated with thrombin (100 μ g) in 0.1 M NaCl, 0.02 M Tris (tris(hydroxymethyl)aminomethane)-HCl (pH 7.4) containing 5 mM EDTA (ethylenediaminetetraacetic acid) for 2 h at 37 °C. Resultant activated protein C derivatives were separated from thrombin by fast-protein liquid chromatography using a Mono Q column developed with 40 mL linear gradient from 0.1 to 1.0 M NaCl, in 0.02 M Tris-HCl (pH 7.4) as described.²¹ Partially and fully γ -carboxylated APC derivatives were eluted from the Mono Q column as two distinct peaks at approximately 0.3 and 0.4 M NaCl, respectively, as described.²¹ The APC concentrations were determined from the absorbance at 280 nm assuming a molecular weight of 56 200 and an extinction coefficient ($E_{1\text{cm}}^{1\%}$) of 14.5,²⁵ by amidolytic activity assay using SpPCa, and by stoichiometric titration of enzymes with known concentration of protein C inhibitors as described previously.²¹

Inactivation of APC. Inactivation of APC was achieved following overnight incubation with a 10-fold molar excess of EGR-CK at room temperature in 0.1 M Tris, pH 7.5, 0.1% poly(ethylene glycol), 150 mM NaCl. Unreacted EGR-CK was removed by dialysis in Hepes-buffered saline (HBS)-buffer (20 mM HEPES, pH 7.2, 0.1 M NaCl, 0.01% Tween 20) at 4 °C (two buffer changes). Less than 0.5% of the initial APC activity remained as determined by amidolytic activity using the chromogenic substrate S-2366.

Real-Time Biomolecular Interaction Analysis. The kinetics of the EGR-modified APC (EGR-APC) mutant interactions with FVIII LC or FVIIIa A1/A3C1C2 were determined by SPR-based assay at 37 °C using a BIAcore T-200 instrument (GE Healthcare, Uppsala, Sweden). FVIII LC or FVIIIa A1/A3C1C2 was covalently coupled to the surface of a CM5 chip at a coupling density of approximately 17 or 8.5 ng/mm², respectively. Binding (association) of each EGR-APC mutant was monitored in HBS-buffer containing 5 mM CaCl₂ for 2 min at a flow rate 10 μ L/min. The dissociation of bound EGR-APC mutant was recorded over a 2 min period by changing the EGR-APC mutant-containing buffer to buffer alone. The level of nonspecific binding, corresponding to EGR-APC mutant binding to the uncoated chip, was subtracted from the signal. After each analysis, chip surfaces were regenerated by treatment with 2 M NaCl for 2 min. K_d values were determined by an equilibrium method using the evaluation software provided by GE Healthcare.

FXa Generation Assay. The rate of conversion of FX to FXa was monitored in a purified system.²⁶ FVIII (150 nM) in HBS-buffer containing 5 mM CaCl₂, 100 μ M PSCPE vesicles, and 100 μ g/mL BSA was activated by the addition of thrombin (30 nM). Thrombin activity was inhibited after 1 min by the addition of hirudin (10 units/mL), and the resultant FVIIIa was reacted with each APC mutant (3 nM). Reactions were run at 37 °C. Aliquots were removed at the indicated times to assess residual FVIIIa activity. FXa generation was initiated by the addition of FIXa (40 nM) and FX (300 nM) into the reaction mixture at 23 °C. The reactions were quenched after 1 min by adding 50 mM EDTA. Amounts of FXa generated were determined by addition of the chromogenic substrate Pefachrome Xa (0.46 mM final concentration) at 23 °C, and rates of FXa generation were calculated. FVIIIa activity was determined as the amount of FXa generated per minute, and

this value was used to determine the concentration of active FVIIIa.

Control experiments assessing FVIIIa stability were performed in the absence of APC in order to determine the rates of FVIIIa inactivation resulting from A2 subunit dissociation. At the concentrations of FVIIIa used in reactions, this value approximated an ~15% loss of the initial activity for the 20 min time course. Therefore, for each time point in the time course experiments including APC, the obtained activity was corrected for the contribution of activity loss by the APC-independent mechanism.

Cleavage of FVIIIa by APC. FVIIIa (130 nM) was incubated with each APC mutant (3 nM) in HBS-buffer containing 5 mM CaCl₂, PSCPE (100 μM), and BSA (100 μg/mL) at 37 °C. Samples were taken at the indicated times, and the reactions were immediately terminated and prepared for SDS-PAGE by adding SDS-PAGE sample buffer and boiling for 3 min.

Electrophoresis and Western Blotting. SDS-PAGE was performed using 10% gels at 175 V for 50 min. For Western blotting, the proteins were transferred to a PVDF membrane at 100 V for 1 h in buffer containing 10 mM CAPS [3-(cyclohexylamino)-1-propanesulfonic acid], pH 11 and 10% (v/v) methanol. Proteins were probed with anti-A1 domain monoclonal antibody (S8.12), followed by goat antimouse alkaline phosphatase-linked second antibody. The signal was detected using the ECF system (Amersham Biosciences), and the blots were scanned at 570 nm using a Storm 860 instrument (Molecular Devices). Densitometric scans were quantitated using ImageJ 1.34 (National Institutes of Health).

Data Analysis. All experiments were performed at least three separate times, and mean values and standard deviations are shown. Nonlinear least-squares regression analyses were performed by Kaleidagraph (Synergy, Reading, PA).

Rates of FVIIIa cleavage by APC mutants as determined from Western blotting, and rates of FVIIIa inactivation as determined from FXa generation assays were obtained from curve fitting using a second-order polynomial equation (eq 1), as previously employed.²⁷

$$[\text{FVIIIa}] = A + Bt + Ct^2 \quad (1)$$

where [FVIIIa] is the FVIIIa concentration in nM, *t* is the time in min, *A* is the initial concentration in nM of FVIIIa, and *B* represents the slope value at time zero. The absolute value of *B* is the rate of FVIIIa inactivation that was normalized by APC concentration. The results are expressed in nM FVIIIa/min/nM APC. Initial time points (up to 10 min) or up to ~40% of substrate utilized were used for these analyses.

Values for *K_m* were calculated by fitting the data using a nonlinear least-squares regression analysis to the Michaelis–Menten equation (eq 2) from FXa generation assays.

$$v = V_{\text{max}}[\text{FVIIIa}]/(K_{\text{m}} + [\text{FVIIIa}]) \quad (2)$$

where *v* is the initial velocity in nM and [FVIIIa] is the concentration of FVIIIa in nM.

RESULTS

Expression and Purification of Recombinant APC. In an earlier study, we reported that the basic residues of all three surface loops (39, 60, and 70–80) in APC showed variable effects in modulating the proteolytic inactivation of FVIIIa.¹⁷ The current study was undertaken to assess the contributions of

these residues within APC exosite loops to binding FVIIIa and monitor their effects on rates of cleavage and inactivation. For these studies, a series of recombinant APC proteins were prepared with individual residues within the 39-loop (Lys38 and Lys39), 60-loop (Lys62, Lys63, and Arg67), and 70–80-loop (Arg74, Arg75, and Lys78) replaced with Ala as previously described.¹⁷ Expression, purification, and activation of protein C mutants by thrombin have been described previously.^{21,22} The amidolytic activity and the anticoagulant function of these APC mutants were evaluated by both clotting and FVa degradation assays as previously described.^{21,28,29} All APC mutants showed normal amidolytic activities with the exception of the Arg67Ala mutant, which was somewhat impaired.¹⁷ Thus, conclusions regarding this variant are tentative. The Lys37Ala variant was refractory to proper γ-carboxylation and thus was not further studied. The rationale for substitution of corresponding residues of thrombin for Lys37–Lys39 of APC was based on the observation that these proteases have the greatest structural similarities among the coagulation proteases and that such substitution would likely minimally affect the structure of the mutant protein.

Binding of APC Mutants to FVIII LC or FVIIIa A1/A3C1C3. The FVIII A1 domain³⁰ and LC³¹ have been shown to contain interactive sites for APC. For this reason we employed two FVIII substrates for binding studies using SPR. The first, the isolated FVIII LC is comprised of A3C1C2 domains, whereas the second substrate, the FVIIIa A1/A3C1C2 dimer, contains the A1 domain in tight association with the LC-derived A3C1C2 subunits. Both reagents contain a segment of acidic rich residues. In the LC, this segment is represented by a3 (residues 1649–1689) that is cleaved and removed during the activation of FVIII to FVIIIa. In the FVIIIa A1/A3C1C2 dimer, the acidic segment is represented by a1 (residues 337–372), which is located at the C-terminal end of the A1 subunit. We employed the dimer rather than the complete FVIIIa trimer (A1/A2/A3C1C2) because of the tendency for the A2 subunit to dissociate. These substrates were immobilized onto CM5 sensor chips as described in Materials and Methods, and binding analyses utilized the active site-modified EGR-APC reagents in the fluid phase. The DEGR-APC WT as well as the variants interacted with low affinity to the A1/A3C1C2 dimer and FVIII LC, and it was difficult to obtain reliable *K_d* values from the kinetic parameters. Therefore, maximum response units (RU) determined following addition of various concentrations of EGR-APC variants were used for calculation. These RU values increased in a concentration-dependent manner, and the data were well-fitted using a single-site binding model (see Supporting Information Figure 1S). The results from this analysis are summarized in Table 1. The *K_d* values for wild-type APC binding to the FVIIIa A1/A3C1C2 dimer and FVIII LC were 525 ± 32 and 546 ± 142 nM, respectively. These values were essentially equivalent, suggesting that the clustered acidic residues in the two substrates may make similar contributions to the APC binding site(s). Furthermore, Lys39Ala, Lys-Lys-Lys/Pro-Gln-Glu, Lys63Ala, and Arg67Ala variants showed significant increases (4.4–10.2-fold) in *K_d* compared to the wild-type value in binding to the two substrates, suggesting that these residues may directly participate in the binding interactions.

Inactivation of FVIIIa by APC Mutants. FVIII (150 nM) was activated by thrombin (30 nM). The resultant FVIIIa was reacted with 3 nM of each APC mutant in the presence of 100 μM PSCPE vesicles. The reactions were then initiated with

Table 1. Binding Parameters for the Interaction of APC Mutants and FVIII Subunits by SPR^a

APC form	K_d (nM)	
	FVIIIa A1/A3C1C2	FVIII LC
WT	546 ± 142 (1.0)	525 ± 32 (1.0)
Lys38Ala	918 ± 93 (1.7)	240 ± 26 (0.5)
Lys39Ala	2099 ± 90 (3.9)	2471 ± 270 (4.7)
Lys-Lys-Lys/Pro-Gln-Glu	3474 ± 196 (6.4)	5344 ± 520 (10)
Lys62Ala	899 ± 134 (1.6)	1483 ± 150 (2.8)
Lys63Ala	1350 ± 320 (2.5)	2286 ± 280 (4.4)
Arg67Ala	2306 ± 600 (4.2)	2917 ± 110 (5.6)
Arg74Ala	1191 ± 150 (2.2)	584 ± 120 (1.1)
Arg75Ala	2119 ± 340 (3.9)	1177 ± 170 (2.2)
Lys78Ala	738 ± 66 (1.4)	1109 ± 96 (2.1)

^aReactions were performed as described under Materials and Methods. Parameter values ± standard deviations were calculated by nonlinear regression analysis using the evaluation software provided by GE Healthcare. Values in parentheses are kinetic parameter values relative to wild-type.

300 nM FX and 40 nM FIXa, and cofactor activity was monitored for 20 min using a FXa generation assay as described in Materials and Methods (Figure 1). The values for cofactor

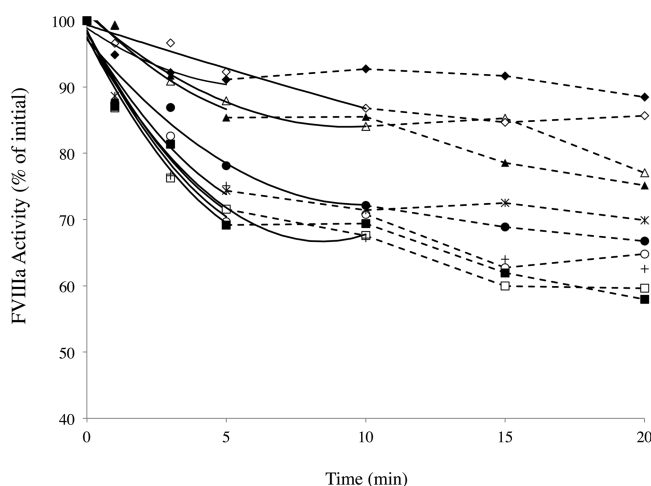


Figure 1. Inactivation of FVIIIa by APC mutants. FVIII (150 nM) was activated by thrombin (30 nM). FVIIIa inactivation was then monitored over time in the presence of each APC mutant (3 nM) using a FXa generation assay. APC-catalyzed inactivation values were corrected by subtracting the corresponding values for FVIIIa decay obtained in the absence of APC. Solid lines were drawn from the curve fitting as described in the Materials and Methods with dashed lines connecting points not used for determination of parameter values. The symbols used are as follows: wild-type (open circles), Lys38Ala (closed circles), Lys39Ala (open triangles), Lys-Lys-Lys/Pro-Gln-Glu (closed triangles), Lys62Ala (open squares), Lys63Ala (closed squares), Arg67Ala (open diamonds), Arg74Ala (closed diamonds), Arg75Ala (crosses), and Lys78Ala (asterisks). Experiments were performed at least three separate times, and mean values are shown.

inactivation rates were derived from the curve fits from the initial 5 or 10 min of the reactions. High concentrations of FVIIIa (150 nM) were used to minimize inactivation due to dissociation of A2 subunit from the A1/A3C1C2 dimer. The observed loss of FVIIIa activity obtained in the absence of APC was similar for the all variants and wild-type FVIIIa forms (~10% activity loss at 20 min, data not shown), and this value

was used as a correction factor in determining APC-dependent inactivation rates. Lys38Ala, Lys62Ala, Lys63Ala, Arg75Ala, and Arg78Ala variants showed similar rates of inactivation as the wild-type APC. Inactivation rates for Lys39Ala, Lys-Lys-Lys/Pro-Gln-Glu, Arg67Ala, and Arg74Ala variants were all reduced to varying degrees ranging from ~20 to ~55% the wild-type value (Table 2), suggesting that these residues may make more

Table 2. Rates of FVIIIa Inactivation and A1 Subunit Cleavage by Wild-Type and Mutant APC^a

APC form	inactivation (nM FVIIIa/min/nM APC)	A1 cleavage (nM A1/min/nM APC)
WT	6.7 ± 1.2 (1.00)	6.8 ± 0.8 (1.00)
Lys38Ala	5.0 ± 1.9 (0.75)	4.8 ± 1.1 (0.71)
Lys39Ala	3.6 ± 0.7 (0.54)	0.7 ± 0.1 (0.10)
Lys-Lys-Lys/ Pro-Gln-Glu	2.2 ± 0.4 (0.33)	0.0 ± 0.0 (0.00)
Lys62Ala	8.1 ± 1.5 (1.21)	2.3 ± 0.4 (0.33)
Lys63Ala	7.5 ± 1.4 (1.12)	2.0 ± 0.4 (0.29)
Arg67Ala	1.4 ± 0.7 (0.21)	0.5 ± 0.3 (0.07)
Arg74Ala	1.8 ± 0.6 (0.27)	0.4 ± 0.3 (0.06)
Arg75Ala	7.3 ± 1.8 (1.09)	5.7 ± 1.1 (0.83)
Lys78Ala	7.1 ± 1.1 (1.06)	2.8 ± 0.4 (0.40)

^aRates of FVIIIa inactivation and A1 cleavage were estimated by nonlinear least-squares regression analysis from the data shown in Figures 1 and 2, respectively, using eq 1 as described under Materials and Methods. Data points represent mean ± standard deviations from at least three separate experiments. Values in parentheses are kinetic parameter values relative to wild-type.

prominent contribution to the interaction of enzyme with substrate than other residues within the APC exosite. These results suggest that a number of residues within the 39-, 60-, and 70–80-loops make a moderate contribution to inactivation of FVIIIa by APC and that there may be an overall limit to this contribution in effecting reaction rate.

Cleavage of FVIIIa by APC Variants. Western blotting was performed to monitor the rates of APC-catalyzed proteolysis at Arg³³⁶, the primary site for cleavage in the FVIIIa substrate, and correlate this event with the reduced rates of FVIIIa inactivation. FVIIIa (130 nM) was incubated with APC variants (3 nM) and PSCPE vesicles (100 μM), and the reactions were quenched at specified intervals as described in Materials and Methods. Intact A1 (A1^{1–372}) and the product of proteolysis (A1^{1–336}) were visualized by Western blotting (Figure 2a) using a monoclonal antibody (58.12) that recognizes the N-terminal sequence of the A1 domain. Scanning densitometry obtained from the blots was employed to quantitate band densities of the A1 substrate. Density values for A1 substrate and product were normalized to the FVIIIa concentration, and nonlinear least-squares regression analysis was performed to calculate the rates of cleavage (Figure 2b). The values derived from curve fits were determined from the initial 10 min of the reactions which are presented in Table 2.

Similar to the cofactor inactivation results, cleavage rates of A1 subunit at Arg³³⁶ for all variants were reduced to variable extents with the Lys39Ala, Lys-Lys-Lys/Pro-Gln-Glu, Arg67Ala, and Arg74Ala variants showing the greatest reductions (~10% of the wild-type value) in rate (Table 2). Together, results from the cofactor inactivation and A1 cleavage experiments suggest that all exosite loops in APC contribute to the efficient inactivation of FVIIIa with residues Lys39 of the 39-loop, Arg67 of the 60-loop, and Arg74 of the 70–80-loop representing

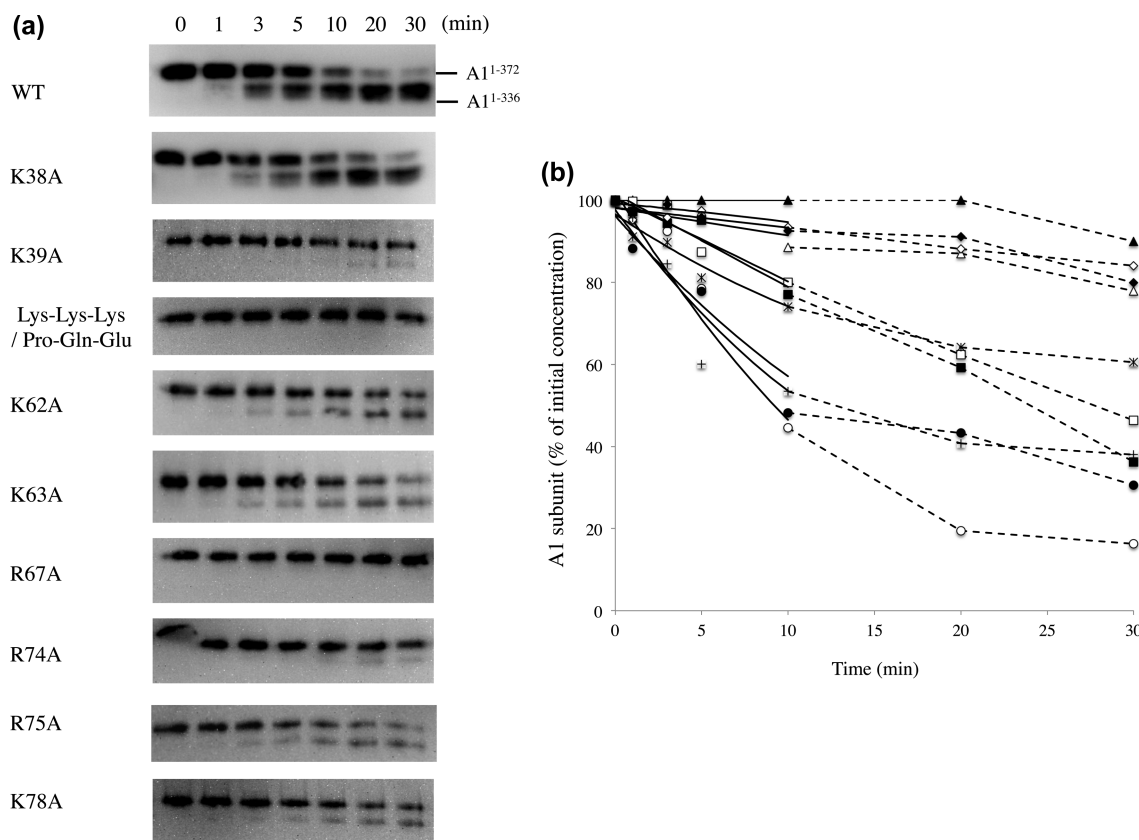


Figure 2. A1 subunit cleavage rates of the FVIIIa by APC mutants. (a) FVIIIa (130 nM) was activated by thrombin (30 nM) and then reacted with each APC mutant (3 nM). Aliquots were taken at indicated time points (0–30 min) and were subjected to SDS-PAGE. A1 substrate and A1^{1–336} product are visualized by Western blotting using the 58.12 monoclonal antibody. (b) Loss of A1 subunit for each reaction was calculated based on the band density values and plotted as a function of time. Lines were drawn from the curve fitting of second order polynomial equation (eq 1) as described under the Materials and Methods. The symbols used are as follows: wild-type (open circles), Lys38Ala (closed circles), Lys39Ala (open triangles), Lys-Lys-Lys/Pro-Gln-Glu (closed triangles), Lys62Ala (open squares), Lys63Ala (closed squares), Arg67Ala (open diamonds), Arg74Ala (closed diamonds), Arg75Ala (crosses), and Lys78Ala (asterisks). Experiments were performed at least three separate times, and typical results are shown.

prominent determinants within this sequence for interaction with FVIIIa.

Michaelis–Menten Analysis of APC-Catalyzed Inactivation of FVIII. The kinetic parameters K_m and V_{max} for FVIIIa inactivation catalyzed by the APC variants were determined by titrating FVIIIa and assessing residual cofactor activity in a FXa generation assay. Various concentrations of FVIII (0–1000 nM) were activated to FVIIIa by thrombin as described in Materials and Methods with subsequent addition of hirudin to quench thrombin activity. The FVIIIa generated was immediately reacted with APC variants (3 nM). Aliquots were removed at the indicated times, and cofactor activity was monitored using a FXa generation assay as described in Materials and Methods. Generated FXa was used to estimate the initial velocity of FVIIIa cleavage by APC, and these data were plotted against FVIIIa concentration and fitted to the Michaelis–Menten equation. Results are presented in Figure 3 and summarized in Table 3. With the exception of the Lys38Ala, Lys63Ala, and Arg75Ala variants, K_m values for all the variants tested were somewhat increased with the Lys39Ala, Arg67Ala, and Arg74Ala variants demonstrating the greatest increases (~2.6–4.0-fold) compared to wild-type APC. Furthermore, the Lys-Lys-Lys/Pro-Gln-Glu triple mutant showed a very similar increase (4.4-fold relative to WT) in K_m compared to that observed for the Lys39Ala point mutant

(4.1-fold), suggesting that Lys39 is the dominant residue in regulating substrate binding. On the other hand, V_{max} values were largely unaffected by the mutations with most values within ~20% of the wild-type value. Exceptions were Lys39Ala and the triple mutant which demonstrated an ~1.8-fold increase in V_{max} . The reason(s) for this modest increase in rate is unclear. Overall, these kinetic data are consistent with results observed for binding in the absence of catalysis and indicate that at least one basic residue of each loop and in particular residues Lys39, Arg67, and Arg74 within these exosite loops contribute to binding substrate.

DISCUSSION

Protein C is a single chain vitamin K-dependent zymogen for a plasma serine protease that upon activation by the complex of the thrombin–thrombomodulin downregulates the coagulation cascade by limited proteolysis of FVa and FVIIIa.^{32–34} Structural data have identified three surface loops (39, 60, and 70–80), rich in basic residues, located in the protease domain of APC near the active site pocket¹⁶ (see Figure 4). Both A1 and A2 subunits of FVIIIa contain acidic C-terminal sequences that may potentially provide interactive sites for the basic exosite of APC.^{17,30} Furthermore, the a3 segment in the isolated FVIII LC also provides a potential exosite-interactive region that is present in FVIII but not in FVIIIa. The similar

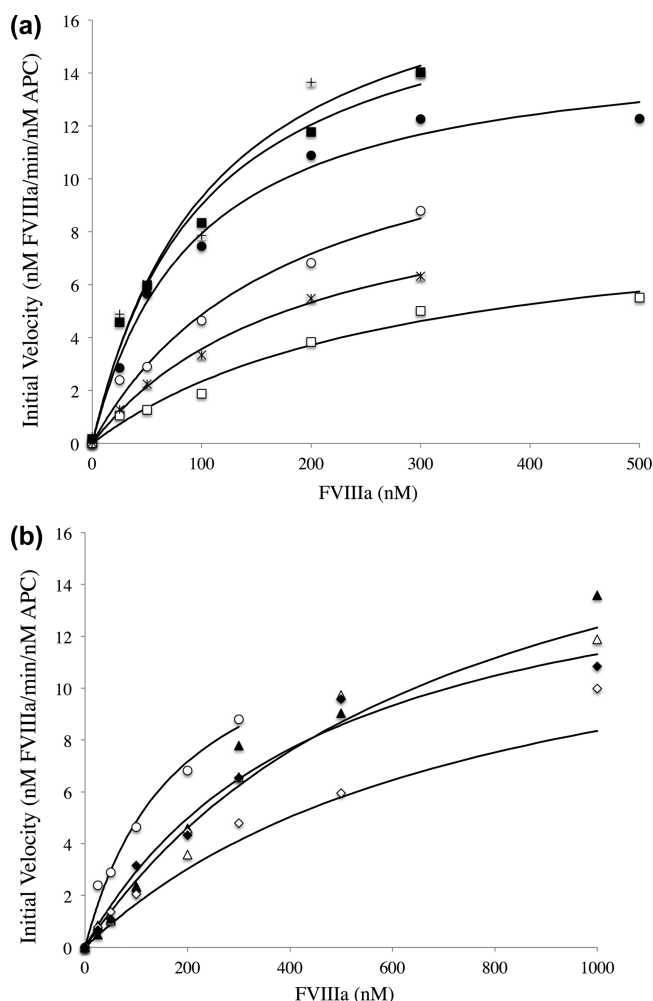


Figure 3. Concentration dependence of FVIIIa degradation by APC variants as determined by factor Xa generation assays. (a, b) Inactivation rates for FVIIIa was determined at various concentrations of FVIIIa (0–1000 nM) as described in Materials and Methods. Loss of FVIIIa activity was calculated based on FXa generation assays. Analysis of inactivation velocity by APC was performed using a curve fitting of second-order polynomial equation (eq 1). Data were fitted to Michaelis–Menten equation (eq 2) using nonlinear regression analysis as described in Materials and Methods. The symbols used are as follows: wild-type (open circles), Lys38Ala (closed circles), Lys39Ala (open triangles), Lys-Lys-Lys/Pro-Gln-Glu (closed triangles), Lys62Ala (open squares), Lys63Ala (closed squares), Arg67Ala (open diamonds), Arg74Ala (closed diamonds), Arg75Ala (crosses), and Lys78Ala (asterisks). Experiments were performed at least three separate times, and mean values are shown.

affinity values for the APC WT and variants as determined for the A1/A3C1C2 dimer and LC are consistent with utilization of the a1 and a3 segments in the respective substrates for exosite binding.

Earlier results from our laboratory identified a sequence in LC (A3 domain) comprised of residues 2007–2016 that was interacting with APC.³⁵ This sequence is defined by ²⁰⁰⁷His-Gly-Ala-Ser-Thr-Leu-Phe-Leu-Val²⁰¹⁶. While this region likely interacts with APC via electrostatic and/or hydrophobic interaction, it lacks acidic residues with which to form salt linkages with the basic residues of the APC exosite. Thus, we predict that this region of FVIII LC does not comprise an exosite-interactive region.

Table 3. Michaelis–Menten Parameters for APC-Catalyzed Inactivation of FVIIIa^a

APC form	K_m (nM)	V_{max} (nM min ^{−1})
WT	179 ± 48	13.6 ± 1.8
Lys38Ala	92.6 ± 14.1	15.2 ± 0.8
Lys39Ala	721 ± 198	21.2 ± 3.3
Lys-Lys-Lys/Pro-Gln-Glu	788 ± 168	24.3 ± 3.0
Lys62Ala	286 ± 82	9.0 ± 1.3
Lys63Ala	101 ± 21	18.1 ± 1.5
Arg67Ala	681 ± 185	16.2 ± 2.4
Arg74Ala	466 ± 103	16.6 ± 1.8
Arg75Ala	110 ± 38	19.5 ± 2.8
Lys78Ala	193 ± 25	10.5 ± 0.7

^aReactions were performed as described under Materials and Methods. K_m and V_{max} values ± standard deviations were calculated by Michaelis–Menten kinetics.

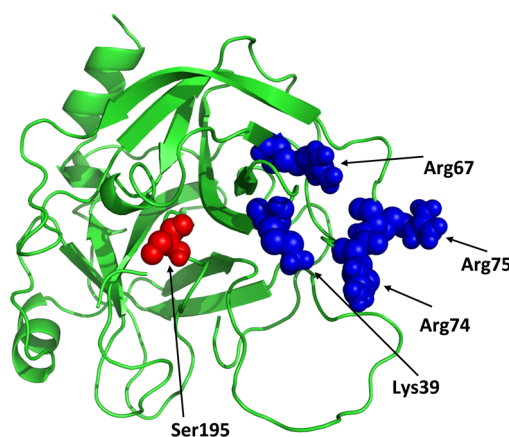


Figure 4. Localization of the proposed FVIII binding site in the three-dimensional structure of APC. Relative three-dimensional locations of side chains of the basic residues (blue) of the three surface loops 39, 60, and 70–80 are shown. The active site Ser195 is shown in red. Coordinates (Protein Data Bank entry 1AUT) were used to prepare the figure.¹⁶

SPR analysis of the APC point mutations yielded some interesting observations. For example, the triplet Lys residues 37–39 appear important in binding FVIII substrate as judged by the marked increase in K_d when this sequence was replaced *en bloc* with the homologous sequence from thrombin (Pro-Gln-Glu). However, replacing Lys38 and Lys39 individually with Ala yielded significant differences in binding interactions. While the replacement of Lys38 yielded little effect, replacement of Lys39 accounted for approximately half the reduction in affinity observed with the Lys-Lys-Lys/Pro-Gln-Glu variant, consistent with this residue having a major contribution to binding. Unfortunately, we were unable to assess the role of the Lys37Ala variant in this interaction as it was refractory to proper γ -carboxylation.

Two other residues appeared to make dominant contributions compared with other residues in the APC surface loops. Comparing Ala variants for 60-loop residues Lys62, Lys63, and Arg67, the latter variant, Arg67Ala, showed ~2–3-fold greater increases in K_d compared with the Lys62Ala variant dependent upon the FVIII substrate utilized, while the Lys63Ala variant yielded K_d values that were somewhat intermediate. Alternatively, with regard to the 70–80-loop, Arg75Ala exhibited K_d values that were ~2- and ~3-fold greater than Arg74Ala and

Lys78Ala when tested with the FVIIIa A1/A3C1C2 substrate. This variant also demonstrated an ~2-fold increase in K_d compared with Arg74Ala on the FVIII LC substrate, while showing a similar K_d value to the Lys78Ala with this substrate. Overall, these results tend to suggest that a dominant residue with respect to binding is found in each loop forming the APC exosite. These residues are highlighted in Figure 4.

In an earlier study,¹⁷ we examined a number of these APC variants including the 60- and 70–80-loop variants used in this report in functional studies assessing both inactivation FVIIIa and cleavage of the A1 subunit by the variants. These studies were limited in that rate values for either functional parameter were not determined. Furthermore, while the Lys-Lys-Lys/Pro-Gln-Glu variant was available for evaluation, neither the Lys38Ala nor Lys39Ala point mutants were available, thus limiting our conclusions related to the 39-loop residues. In the present study, rate values for A1 subunit cleavage as well as for APC-catalyzed inactivation of FVIIIa by each APC variant were determined by time course reactions using Western blotting and FXa generation assays, respectively. Consistent with our earlier results, a dominant role for the 39-loop was suggested by an ~70% reduction in the rate of FVIIIa inactivation by the Lys-Lys-Lys/Pro-Gln-Glu variant. This variant also showed essentially no cleavage of the A1 subunit, suggesting cofactor inactivation derived in large part from cleavage of the A2 site. Consistent with its apparent role in binding substrate, the Lys39 residue demonstrated the greatest effect in reducing cleavage (~10% the WT value) and inactivation (~50% the WT value) rates when this residue was replaced with Ala. In addition, prominent effects on function were observed for the Arg67Ala and Arg74Ala variants, and these results were similar to the earlier report. The observation that the Arg74Ala variant showed a greater effect on functional parameters while the Arg75Ala exhibited a somewhat greater defect in binding the FVIII substrates suggests a possible direct effect of Arg74 in the catalytic mechanism.

In an earlier report, Yang et al.²¹ demonstrated that the basic residues of the 39-, 60-, and 70–80-loop of APC were part of the heparin-binding site of the protease and suggested that Arg74 and Arg75 might constitute a direct binding site for FVa and possibly FVIIIa. Our results are consistent with this prediction. In the case of the 60-loop, mutagenesis studies have demonstrated that Lys62 and Lys63 residues which contribute to the heparin-binding site are important for heparin-mediated stimulation of inhibition of APC by protein C inhibitor.³⁶ On the other hand, our results show that Arg67 plays an important role in the binding of APC to FVIII LC. Taken together, these observations support the notion that the 60-loop is especially important for the regulation of coagulation.

In addition to basic residues of these loops (39, 60, and 70–80), the autolysis loop (148-loop) of APC is also highly basic, with 5 basic and 2 acidic residues.¹⁶ An alanine scanning study of the autolysis loop showed that basic residues Arg147, Lys149c, Arg149d, and Arg151 were the most important residues for the interaction of APC with FVa.³⁷ Recently, Cramer et al.³⁸ have demonstrated that basic residues Arg147, Lys149c, and Arg151 are essential for FVIIIa inactivation by APC. These results show that the autolysis loop also plays a significant role as part of the basic exosite on APC in the interaction with FVIIIa. Based on the 3D structure of the APC serine protease domain,¹⁶ Lys39 and Arg67, and Arg74 are the closest residues in each loop to the autolysis loop. Taken together, these observations suggest that these three residues

contribute to the inactivation of FVIIIa and may cooperate with residues within the autolysis loop.

In conclusion, we demonstrate a role for selected residues in forming an FVIII(a)-interactive site within the 39-, 60-, and 70–80-loops of APC. At least one residue from each loop significantly contributes to interaction with substrate FVIIIa. Specifically, Lys39, Arg67, and Arg74/Arg75 make key contributions to the FVIII(a) binding interaction and/or FVIIIa inactivation by cleavage at Arg³³⁶. Thus, the three loops form an exosite that is critical for optimal interaction with the FVIIIa substrate.

■ ASSOCIATED CONTENT

● Supporting Information

Binding of selected APC mutants to FVIII LC by SPR (Figure S1); maximum RU values at equilibrium for association of APC mutants plotted as a function of APC mutant concentration, and the data fit using eq 2 according to a single-site binding model; experiments performed at least three separate times and mean values shown; symbols used: wild-type (open circles), Lys39Ala (closed circles), Lys-Lys-Lys/Pro-Gln-Glu (open triangles), Lys63Ala (closed triangles), and Arg67Ala (open squares). This material is available free of charge via the Internet at <http://pubs.acs.org>.

■ AUTHOR INFORMATION

Corresponding Author

*Tel 585-275-6576; Fax 585-275-6007; e-mail philip_fay@urmc.rochester.edu.

Present Address

[§]M.T.: Department of Pediatrics, Nara Medical University, Kashihara, Nara 634-8522, Japan.

Funding

This work was supported by National Institutes of Health Grants HL76213 and HL38199 (to P.J.F.) and HL101917 and HL62565 (to A.R.R.)

Notes

The authors declare no competing financial interest.

■ ACKNOWLEDGMENTS

We thank Lisa Regan for the gifts of recombinant FVIII (Kogenate) and the 58.12 monoclonal antibody.

■ ABBREVIATIONS

F, factor; LC, light chain; HC, heavy chain; VWF, von Willebrand factor; APC, activated protein C; Lys-Lys-Lys/Pro-Gln-Glu, a triple mutant of APC where Lys37, Lys38, and Lys39 are replaced with Pro, Gln, and Glu, respectively; DEGR, 1,5-dansyl-Glu-Gly-Arg; EGR-CK, 1,5-Glu-Gly-Arg chloromethyl ketone; SDS-PAGE, sodium dodecyl sulfate–polyacrylamide gel electrophoresis; HEPES, 4-(2-hydroxyethyl)-1-piperazineethanesulfonic acid; CAPS, 3-(cyclohexylamino)-1-propanesulfonic acid; SPR, surface plasmon resonance; ELISA, enzyme-linked immunosorbent assay; BSA, bovine serum albumin; PVDF, poly(vinylidene difluoride).

■ REFERENCES

- (1) Mann, K. G., Nesheim, M. E., Church, W. R., Haley, P., and Krishnaswamy, S. (1990) Surface-dependent reactions of the vitamin K-dependent enzyme complexes. *Blood* 76, 1–16.

- (2) Vehar, G. A., Keyt, B., Eaton, D., Rodriguez, H., O'Brien, D. P., Rotblat, F., Oppermann, H., Keck, R., Wood, W. I., Harkins, R. N., et al. (1984) Structure of human factor VIII. *Nature* 312, 337–342.
- (3) Andersson, L. O., Forsman, N., Huang, K., Larsen, K., Lundin, A., Pavlu, B., Sandberg, H., Sewerin, K., and Smart, J. (1986) Isolation and characterization of human factor VIII: molecular forms in commercial factor VIII concentrate, cryoprecipitate, and plasma. *Proc. Natl. Acad. Sci. U. S. A.* 83, 2979–2983.
- (4) Fay, P. J., Anderson, M. T., Chavin, S. I., and Marder, V. J. (1986) The size of human factor VIII heterodimers and the effects produced by thrombin. *Biochim. Biophys. Acta* 871, 268–278.
- (5) Eaton, D., Rodriguez, H., and Vehar, G. A. (1986) Proteolytic processing of human factor VIII. Correlation of specific cleavages by thrombin, factor Xa, and activated protein C with activation and inactivation of factor VIII coagulant activity. *Biochemistry* 25, 505–512.
- (6) Fay, P. J., Matri, M., Koszelak, M. E., and Wakabayashi, H. (2001) Cleavage of factor VIII heavy chain is required for the functional interaction of A2 subunit with factor IXa. *J. Biol. Chem.* 276, 12434–12439.
- (7) Lollar, P. (1991) The association of factor VIII with von Willebrand factor. *Mayo Clinic proceedings. Mayo Clinic* 66, 524–534.
- (8) Regan, L. M., and Fay, P. J. (1995) Cleavage of factor VIII light chain is required for maximal generation of factor VIIIa activity. *J. Biol. Chem.* 270, 8546–8552.
- (9) Fay, P. J. (2004) Activation of factor VIII and mechanisms of cofactor action. *Blood Rev.* 18, 1–15.
- (10) Fay, P. J., Beattie, T. L., Regan, L. M., O'Brien, L. M., and Kaufman, R. J. (1996) Model for the factor VIIIa-dependent decay of the intrinsic factor Xase. Role of subunit dissociation and factor IXa-catalyzed proteolysis. *J. Biol. Chem.* 271, 6027–6032.
- (11) Fay, P. J., Smudzin, T. M., and Walker, F. J. (1991) Activated protein C-catalyzed inactivation of human factor VIII and factor VIIIa. Identification of cleavage sites and correlation of proteolysis with cofactor activity. *J. Biol. Chem.* 266, 20139–20145.
- (12) Plantier, J. L., Rolli, V., Ducasse, C., Dargaud, Y., Enjolras, N., Boukerche, H., and Negrier, C. (2010) Activated factor X cleaves factor VIII at arginine 562, limiting its cofactor efficiency. *J. Thromb. Haemostasis* 8, 286–293.
- (13) Eaton, D. L., Wood, W. I., Eaton, D., Hass, P. E., Hollingshead, P., Wion, K., Mather, J., Lawn, R. M., Vehar, G. A., and Gorman, C. (1986) Construction and characterization of an active factor VIII variant lacking the central one-third of the molecule. *Biochemistry* 25, 8343–8347.
- (14) Wacey, A. I., Pemberton, S., Cooper, D. N., Kakkar, V. V., and Tuddenham, E. G. (1993) A molecular model of the serine protease domain of activated protein C: application to the study of missense mutations causing protein C deficiency. *Br. J. Haematol.* 84, 290–300.
- (15) Fisher, C. L., Greengard, J. S., and Griffin, J. H. (1994) Models of the serine protease domain of the human antithrombotic plasma factor activated protein C and its zymogen. *Protein Sci.* 3, 588–599.
- (16) Mather, T., Oganessyan, V., Hof, P., Huber, R., Foundling, S., Esmon, C., and Bode, W. (1996) The 2.8 Å crystal structure of Glu-domainless activated protein C. *EMBO J.* 15, 6822–6831.
- (17) Manithody, C., Fay, P. J., and Rezaie, A. R. (2003) Exosite-dependent regulation of factor VIIIa by activated protein C. *Blood* 101, 4802–4807.
- (18) O'Brien, L. M., Huggins, C. F., and Fay, P. J. (1997) Interacting regions in the A1 and A2 subunits of factor VIIIa identified by zero-length cross-linking. *Blood* 90, 3943–3950.
- (19) Mimms, L. T., Zampighi, G., Nozaki, Y., Tanford, C., and Reynolds, J. A. (1981) Phospholipid vesicle formation and transmembrane protein incorporation using octyl glucoside. *Biochemistry* 20, 833–840.
- (20) Nogami, K., Lapan, K. A., Zhou, Q., Wakabayashi, H., and Fay, P. J. (2004) Identification of a factor Xa-interactive site within residues 337–372 of the factor VIII heavy chain. *J. Biol. Chem.* 279, 15763–15771.
- (21) Yang, L., Manithody, C., and Rezaie, A. R. (2002) Contribution of basic residues of the 70–80-loop to heparin binding and anticoagulant function of activated protein C. *Biochemistry* 41, 6149–6157.
- (22) Rezaie, A. R. (2001) Vitronectin functions as a cofactor for rapid inhibition of activated protein C by plasminogen activator inhibitor-1. Implications for the mechanism of profibrinolytic action of activated protein C. *J. Biol. Chem.* 276, 15567–15570.
- (23) Wakabayashi, H., Koszelak, M. E., Matri, M., and Fay, P. J. (2001) Metal ion-independent association of factor VIII subunits and the roles of calcium and copper ions for cofactor activity and inter-subunit affinity. *Biochemistry* 40, 10293–10300.
- (24) Ansong, C., and Fay, P. J. (2005) Factor VIII A3 domain residues 1954–1961 represent an A1 domain-interactive site. *Biochemistry* 44, 8850–8857.
- (25) Shen, L., and Dahlback, B. (1994) Factor V and protein S as synergistic cofactors to activated protein C in degradation of factor VIIIa. *J. Biol. Chem.* 269, 18735–18738.
- (26) Lollar, P., Fay, P. J., and Fass, D. N. (1993) Factor VIII and factor VIIIa. *Methods Enzymol.* 222, 128–143.
- (27) Varfaj, F., Wakabayashi, H., and Fay, P. J. (2007) Residues surrounding Arg336 and Arg562 contribute to the disparate rates of proteolysis of factor VIIIa catalyzed by activated protein C. *J. Biol. Chem.* 282, 20264–20272.
- (28) Friedrich, U., Nicolaes, G. A., Villoutreix, B. O., and Dahlback, B. (2001) Secondary substrate-binding exosite in the serine protease domain of activated protein C important for cleavage at Arg-506 but not at Arg-306 in factor Va. *J. Biol. Chem.* 276, 23105–23108.
- (29) Gale, A. J., Tsavaler, A., and Griffin, J. H. (2002) Molecular characterization of an extended binding site for coagulation factor Va in the positive exosite of activated protein C. *J. Biol. Chem.* 277, 28836–28840.
- (30) Varfaj, F., Neuberger, J., Jenkins, P. V., Wakabayashi, H., and Fay, P. J. (2006) Role of P1 residues Arg336 and Arg562 in the activated-Protein-C-catalysed inactivation of Factor VIIIa. *Biochem. J.* 396, 355–362.
- (31) Fay, P. J., and Walker, F. J. (1989) Inactivation of human factor VIII by activated protein C: evidence that the factor VIII light chain contains the activated protein C binding site. *Biochim. Biophys. Acta* 994, 142–148.
- (32) Esmon, C. T. (1993) Molecular events that control the protein C anticoagulant pathway. *Thromb. Haemost.* 70, 29–35.
- (33) Walker, F. J., and Fay, P. J. (1992) Regulation of blood coagulation by the protein C system. *FASEB J.* 6, 2561–2567.
- (34) Kalafatis, M., Rand, M. D., and Mann, K. G. (1994) The mechanism of inactivation of human factor V and human factor Va by activated protein C. *J. Biol. Chem.* 269, 31869–31880.
- (35) Walker, F. J., Scandella, D., and Fay, P. J. (1990) Identification of the binding site for activated protein C on the light chain of factors V and VIII. *J. Biol. Chem.* 265, 1484–1489.
- (36) Shen, L., Villoutreix, B. O., and Dahlback, B. (1999) Involvement of Lys 62(217) and Lys 63(218) of human anticoagulant protein C in heparin stimulation of inhibition by the protein C inhibitor. *Thromb. Haemost.* 82, 72–79.
- (37) Gale, A. J., Heeb, M. J., and Griffin, J. H. (2000) The autolysis loop of activated protein C interacts with factor Va and differentiates between the Arg506 and Arg306 cleavage sites. *Blood* 96, 585–593.
- (38) Cramer, T. J., and Gale, A. J. (2011) Function of the activated protein C (APC) autolysis loop in activated FVIII inactivation. *Br. J. Haematol.* 153, 644–654.